Ring Size in Octreotide Amide Modulates Differently Agonist versus Antagonist Binding Affinity and Selectivity

Christy Rani R. Grace,[‡] Judit Erchegyi,[†] Manoj Samant,[†] Renzo Cescato,[§] Veronique Piccand,[§] Roland Riek,[‡] Jean Claude Reubi,[§] and Jean E. Rivier*,[†]

The Clayton Foundation Laboratories for Peptide Biology and Structural Biology Laboratory, The Salk Institute for Biological Studies, 10010 North Torrey Pines Road, La Jolla, California 92037, and Division of Cell Biology and Experimental Cancer Research, Institute of Pathology, University of Berne, Berne, Switzerland 3012

Received November 15, 2007

H-DPhe^2-c[Cys^3-Phe^7-DTrp^8-Lys^9-Thr^{10}-Cys^{14}]-Thr^{15}-NH_2 (**1**) (a somatostatin agonist, SRIF numbering) and H-Cpa^2-c[DCys^3-Tyr^7-DTrp^8-Lys^9-Thr^{10}-Cys^{14}]-Nal^{15}-NH_2 (**4**) (a somatostatin antagonist) are based on the structure of octreotide that binds to three somatostatin receptor subtypes ($sst_{2/3/5}$) with significant binding affinity. Analogues of **1** and **4** were synthesized with norcysteine (Ncy), homocysteine (Hcy), or D-homocysteine (DHcy) at positions 3 and/or 14. Introducing Ncy at positions 3 and 14 constrained the backbone flexibility, resulting in loss of binding affinity at all sst_s. The introduction of Hcy at positions 3 and 14 improved selectivity for sst_2 as a result of significant loss of binding affinity at the other sst_s. Substitution by DHcy at position 3 in the antagonist scaffold (**5**), on the other hand, resulted in a significant loss of binding affinity at sst_2 and sst_3 as compared to the different affinities of the parent compound (**4**). The 3D NMR structures of the analogues in dimethylsulfoxide are consistent with the observed binding affinities.

Introduction

The development of a strictly somatostatin (SRIF)[a] receptor 2 (sst_2)-selective analogue remains a challenge, because analogues reported with high binding affinity to sst_2 often also bind with high binding affinity to sst_5 and sometimes to sst_3.[1,2] Most of these partially selective analogues are based on the structure of octreotide (H-DPhe^2-c[Cys^3-Phe^7-DTrp^8-Lys^9-Thr^{10}-Cys^{14}]-Thr^{15}-ol, SRIF numbering) and have a type-II′ β-turn in their structure.[3] The nonselective $sst_{2/5}$ pharmacophore requires two aromatic side chains at positions 2 and 7 in addition to the DTrp^8−Lys^9 pair. It has also been shown that octreotide-like analogues undergo conformational changes in their backbone, from β-sheet to α-helix, resulting in two different locations for the Phe/DPhe/Tyr at position 2.[1] This conformational transition complicates the interpretation of a particular structure as the bioactive conformation for a particular receptor (i.e., complicates the definition of the pharmacophore). In fact, it suggests that two conformations are necessary for the analogue to fit into the two different subtype-selective pharmacophores for sst_2 and sst_5. Recently, we published that the replacement of Phe at position 7 by an Ala in the octreotide scaffold resulted in an agonist (H-DPhe^2-c[Cys^3-Ala^7-DTrp^8-Lys^9-Thr^{10}-Cys^{14}]-Thr^{15}-NH_2), which showed unique sst_2 selectivity.[4] Structure−activity relationship (SAR) studies of such analogues suggested that the aromatic side chain at position 7 was not necessary for sst_2 binding but was crucial for sst_3 and sst_5 binding. The 3D structure of this peptide also had a β-turn of type-II′ for the backbone conformation, which oriented the side chain of DTrp^8, the amino alkyl group of Lys^9, and the aromatic ring of DPhe^2 outside the cycle in their respective positions, which were crucial for effective receptor−ligand binding. On the basis of these results, we have proposed an sst_2-selective pharmacophore for the SRIF agonists.[4]

Bass et al. reported that changing the chirality of H-DPhe^2-LCys^3- to H-LPhe^2-DCys^3- in the octreotide scaffold resulted in an SRIF antagonist.[5] Similar to the octreotide-based agonists, these analogues were binding to $sst_{2/5}$ and sometimes to sst_3 as well. On the basis of our SAR studies with sst_2-selective agonists, we have also designed sst_2-selective antagonists having a longer side chain at position 7 (in preparation). The 3D NMR structures of these antagonists identified the pharmacophore for sst_2-selective antagonists, very similar to the pharmacophore for sst_2-selective agonists.[4] Here, we present a novel approach, based on the agonistic and antagonistic octreotide scaffold where the number of the methylene units involved in the disulfide bridge is reduced or increased by the substitutions of Cys at positions 3 and 14 with norcysteine (Ncy) or homocysteine (Hcy). The influence of these modifications on receptor selectivity and binding affinity seems to be different for agonists and antagonists. These data are reported along with the 3D NMR structures of the analogues, which correlate well with the proposed sst_2-selective agonist pharmacophore.

Results

Peptide Synthesis. All of the peptides shown in Table 1 were synthesized automatically on an MBHA resin by using the

* Corresponding author. Phone: (858) 453-4100. Fax: (858) 552-1546. E-mail: jrivier@salk.edu.

† The Clayton Foundation Laboratories for Peptide Biology, The Salk Institute for Biological Studies.

‡ Structural Biology Laboratory, The Salk Institute for Biological Studies.

§ Institute of Pathology, University of Berne.

[a] Abbreviations: The abbreviations for the common amino acids are in accordance with the recommendations of the IUPAC-IUB Joint Commission on Biochemical Nomenclature (*Eur. J. Biochem.* **1984**, *138*, 9–37). The symbols represent the L-isomer except when indicated otherwise. Additional abbreviations: Boc, t-butoxycarbonyl; Bzl, benzyl; Z(2Cl), 2-chlorobenzyloxycarbonyl; CZE, capillary zone electrophoresis; CYANA, combined assignment and dynamics algorithm for NMR applications; DHcy, D-homocysteine; DIC, N,N′-diisopropylcarbodiimide; DIPEA, diisopropylethylamine; DQF-COSY, double quantum filtered correlation spectroscopy; Hcy, homocysteine; HOBt, 1-hydroxybenzotriazole; Mob, 4-methoxybenzyl; Ncy, norcysteine; NOE, nuclear Overhauser enhancement; NOESY, NOE spectroscopy; 3D, three-dimensional; OBzl, benzyl ester; rmsd, root-mean-square deviation; SAR, structure−activity relationship; SRIF, somatostatin; sst_s, SRIF receptors; TEA, triethylamine; TEAP, triethylammonium phosphate; TOCSY, total correlation spectroscopy.

10.1021/jm701445q CCC: $40.75
Published on Web 04/12/2008

Table 1. Physico-chemical Properties, sst_{1-5} Binding Affinities (IC_{50}s, nM), and Functional Studies of the Analogues and Control Peptide Octreotide Amide (**1**)

ID	compd	purity HPLC[a]	purity CZE[b]	MS[c] M_{calc}	MS[c] $M + H_{obs}$	IC_{50} (nM)[d] sst_1	sst_2	sst_3	sst_4	sst_5	no. of atoms in the cycle	sst_2 functional assay sst_2 internalization[e]
	SRIF-28	99	99	3146.5	3147.3	2.2 ± 0.2	2.4 ± 0.2	2.7 ± 0.4	2.7 ± 0.3	2.5 ± 0.2	38	agonist
1[f]	H-DPhe^2-c[Cys^3-Phe^7-DTrp^8-Lys^9-Thr^{10}-Cys^{14}]-Thr^{15}-NH_2 octreotide amide (SRIF numbering)	95	99	1031.4	1032.1	>1000	1.9 ± 0.3	39 ± 14	>1000	5.1 ± 1.1	20	agonist
2	H-DPhe^2-c[Ncy^3-Phe^7-DTrp^8-Lys^9-Thr^{10}-Ncy^{14}]-Thr^{15}-NH_2	99	99	1003.4	1004.3	>1000	337 ± 60	>1000	214 ± 61	>1000	18	nd
3[f]	H-DPhe^2-c[Hcy^3-Phe^7-DTrp^8-Lys^9-Thr^{10}-Hcy^{14}]-Thr^{15}-NH_2	99	99	1059.4	1060.6	>1000	4.9 ± 1.7	452 ± 245	115 ± 34	109 ± 39	22	agonist
4	H-Cpa^2-c[DCys^3-Tyr^7- DTrp^8-Lys^9-Thr^{10}-Cys^{14}]-Nal^{15}-NH_2[28]	99	99	1177.4	1178.4	>1000	5.7 ± 1.5	112 ± 32	296 ± 19	218 ± 63	20	antagonist
5[f]	H-Cpa^2-c[DHcy^3-Tyr^7- DTrp^8-Lys^9-Thr^{10}-Hcy^{14}]-Nal^{15}-NH_2	98	98	1205.4	1205.4	763 ± 208	267 ± 60	359 ± 169	174 ± 41	199 ± 35	22	antagonist

[a] Percent purity determined by HPLC by using buffer system: A = TEAP (pH 2.5) and B = 60% CH_3CN/40% A with a gradient slope of 1% B/min, at a flow rate of 0.2 mL/min on a Vydac C_{18} column (0.21 × 15 cm, 5-μm particle size, 300 Å pore size). Detection at 214 nm. [b] Capillary zone electrophoresis (CZE) was done by using a Beckman P/ACE System 2050 controlled by an IBM Personal System/2 Model 50Z and by using a ChromJet integrator. Field strength of 15 kV at 30 °C, mobile phase: 100 mM sodium phosphate (85:15, H_2O:CH_3CN) pH 2.50, on a Supelco P175 capillary (363 μm OD × 75 μm ID × 50 cm length). Detection at 214 nm. [c] Calculated *m*/*z* of the monoisotope compared with the observed $[M + H]^+$ monoisotopic mass. [d] Values represent the IC_{50} in nM (mean ± SEM, $n \geq 3$). [e] Tested in vitro in HEK-sst_2 cells ($n \geq 2$); nd, not determined. [f] 3D NMR structures of these analogues are presented in this paper.

t-Butoxycarbonyl (Boc) strategy. Boc-Ncy(Mob)-OH, Boc-D/L-Ncy(Mob)-OH,[6] Boc-Hcy(Mob)-OH, and Boc-DHcy-(Mob)-OH were synthesized in our laboratory.[7] The peptides were cleaved and fully deprotected with hydrogen fluoride. Cyclization of the cysteines/norcysteines/homocysteines was mediated by iodine in an acidic milieu.[8]

Purification and Characterization of the Analogues (see Table 1). Purification was carried out by using multiple preparative reversed-phase high-performance liquid chromatography (RP-HPLC) steps.[9] Purity and identity of the analogues were established by analytical RP-HPLC,[9] capillary zone electrophoresis,[10] and mass spectrometry. The purity of the peptides was >95%. The observed monoisotopic mass $(M + H)^+$ values of each peptide matched the calculated mass $(M + H)^+$ values and are given in Table 1.

Receptor Binding. All of the peptides were tested for their ability to bind to the five human SRIF receptor subtypes in competitive experiments by using ^{125}I-[Leu^8,DTrp^{22},Tyr^{25}]SRIF-28 as radioligand. Cell membrane pellets were prepared, and receptor autoradiography was performed as described in detail previously.[11] The binding affinities are expressed as IC_{50} values that are calculated as described previously.[11,12]

We have introduced Ncy and Hcy at positions 3 and 14 to the octreotide scaffold to gain insight into the structure of the peptide and the influence of the number of atoms in the cysteine side chain involved in the disulfide bond on receptor binding and activation. Analogue **2** differs from **1** (a SRIF agonist) in that the two cysteines are substituted by Ncy at positions 3 and 14, resulting in a disulfide bridge with 18 atoms in the cycle instead of 20 atoms. This peptide does not bind to any of the sst_s. Analogue **3** differs from **1** in that the two cysteines are substituted by Hcy at positions 3 and 14, resulting in a disulfide bridge with 22 atoms in the cycle instead of 20 atoms. Whereas **1** binds to the $sst_{2/5}$ receptors with high binding affinity (IC_{50} = 1.9 and 5.1 nM, respectively) and to sst_3 with moderate binding affinity (IC_{50} = 39 nM), **3** binds more selectively to sst_2 with a high binding affinity comparable to that of **1** (IC_{50} = 4.9 nM) but with much less binding affinity to sst_3 and sst_5 (IC_{50} = 452 nM and 109 nM, respectively). On the other hand, **3** also binds to sst_4 to some extent (IC_{50} = 115 nM) (Table 1). Analogue **5** differs from **4** (a reference SRIF antagonist) by the presence of DHcy at position 3 and Hcy at position 14. This analogue binds 50-fold less to sst_2 than **4** (Table 1). 3D structures of **1**, **3**, and **5** were determined by NMR and compared with the sst_2-selective pharmacophore.

Functional Studies: Receptor Internalization. As seen in Table 1, **1** was found to be a potent sst_2 agonist and had no antagonistic properties; **3** was an sst_2 agonist, less potent than **1**, and had no antagonistic properties either; conversely, **4** and **5** had no agonistic properties up to 10 000 nM. However, they were sst_2 antagonists, because they could completely inhibit the [Tyr^3]-octreotide-induced sst_2 internalization.

NMR Studies. In this section, we report the chemical shift assignment of various proton resonances and structural information for the selected analogues **1**,[4] **3**, and **5** (Table 1) by using NMR techniques in the solvent dimethylsulfoxide (DMSO).

Assignment of Proton Resonances, Collection of Structural Restraints, and Structure Determination. The nearly complete chemical-shift assignments of proton resonances (Table S2) for **1**, **3**, and **5** have been carried out by using 2D NMR experiments by applying the standard procedure as described in the Experimental Section. Assignment and structural characterization of **1** (octreotide amide) have been taken from our previously published paper.[4] A large number of experimental nuclear Overhauser enhancements (NOEs) is observed for all of the three analogues in the NOE spectrum (NOESY) measured with a mixing time of 100 ms, leading to over 100 meaningful distance restraints per analogue and concomitantly ~10 restraints per residue (Table 2). These structural restraints are used as input for the structure calculation with the program combined assignment and dynamics algorithm for NMR applications (CYANA)[13] followed by restrained energy minimization by using the program DISCOVER.[14] The resulting bundle of 20 conformers per analogue represents the 3D structure of each analogue in DMSO. For each analogue, the small residual constraint violations in the distances for the 20 refined conformers (Table 2) and the coincidence of the experimental NOEs and short interatomic distances (data not shown) indicate that the input data represent a self-consistent set, and that the restraints are well satisfied in the calculated

Table 2. Characterization of the NMR Structures of the Analogues Studied by NMR[a]

									residual restraint violations on			
						CFF91 energies (kcal/mol)			distances		dihedral angles	
ID#	NOE distance restraints	angle restraints[b]	CYANA target function[c]	backbone rmsd (Å)	overall rmsd (Å)	total energy	van der Waals	electro-static	no ≥ 0.1 Å	max (Å)	no ≥ 1.5°	max (°)
1	115	24	0.002	0.56 ± 0.14	1.06 ± 0.28	210 ± 14	121 ± 10	89 ± 8	0.4 ± 0.1	0.11 ± 0.02	0 ± 0	0 ± 0
3	90	14	0.04	0.70 ± 0.24	1.67 ± 0.34	172 ± 6	113 ± 4	59 ± 3	0.4 ± 0.1	0.15 ± 0.00	0 ± 0	0 ± 0
5	107	15	0.09	0.51 ± 0.27	1.55 ± 0.53	215 ± 4	172 ± 5	43 ± 2	0.7 ± 0.1	0.15 ± 0.03	0 ± 0	0.0 ± 0.05

[a] The bundle of 20 conformers with the lowest residual target function was used to represent the NMR structures of each analogue. [b] Meaningful NOE distance restraints may include intraresidual and sequential NOEs.[1] [c] The target function is zero only if all the experimental distance and torsion angle constraints are fulfilled and all nonbonded atom pairs satisfy a check for the absence of steric overlap. The target function is proportional to the sum of the square of the difference between calculated distance and isolated constraint or van der Waals restraints, and similarly isolated angular restraints are included in the target function. For the exact definition see ref 13.

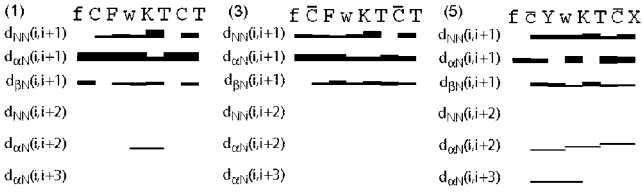

Figure 1. Survey of characteristic NOEs describing the secondary structure of the three analogues studied by NMR (i.e., **1**, **3**, and **5** as indicated). Thin, medium, and thick bars represent weak (4.5−6 Å), medium (3−4.5 Å), and strong (<3 Å) NOEs observed in the NOESY spectrum. The medium-range connectivities $d_{NN}(i, i + 2)$, $d_{\alpha N}(i, i + 2)$, and $d_{\beta N}(i, i + 2)$ are shown by lines starting and ending at the positions of the residues related by the NOE. Residues Hcy, DHcy, DPhe, DTrp, and Nal refer to homocysteine, D-homocysteine, D-phenylalanine, D-tryptophan, and naphthylalanine and are denoted by the symbols, c, C, f, w, and X, respectively.

conformers (Table 2). The deviations from ideal geometry are minimal, and similar energy values are obtained for all of the 20 conformers for each analogue. The quality of the structures determined is furthermore reflected by the small backbone root-mean-square deviation (rmsd) values relative to the mean coordinates of ∼0.5 Å (see Table 2 and Figure 2).

3D Structure of H-DPhe^2-c[Cys^3-Phe^7-DTrp^8-Lys^9-Thr^{10}-Cys^{14}]-Thr^{15}-NH$_2$ (1). Analogue **1** is very similar to octreotide (Thr-ol is substituted by Thr-NH$_2$) and binds to the sst$_{2/3/5}$ receptors with moderately high binding affinity (Table 1). As reported earlier,[4] the torsion angles indicate a type-II′ β-turn conformation for the backbone, as evidenced by the presence of the medium range $d_{\alpha N}(i, i + 2)$ NOE observed between DTrp^8 and Thr^{10} (Figure 1), as well as the hydrogen bond observed between Thr^{10}NH−O′Phe^7 in all of the 20 structures. The unshifted amide proton resonance of Thr^{10} at 7.58 ppm (from 298 to 313K) confirms that this amide proton is involved in a hydrogen bond. The side chain of Phe^7 and DTrp^8 are in the trans rotamer and that of Lys^9 is in the gauche$^+$ rotamer (Table S1).

3D Structure of H-DPhe^2-c[Hcy^3-Phe^7-DTrp^8-Lys^9-Thr^{10}-Hcy^{14}]-Thr^{15}-NH$_2$ (3). Analogue **3** differs from **1** by Hcy at positions 3 and 14 and shows selective binding for sst$_2$ (Table 1). The backbone torsion angles indicate a slightly distorted β-turn of type-II′ conformation around DTrp^8−Lys^9 (Figure 2 and Table S1). The side chains of DPhe^2 and DTrp^8 are in the gauche$^-$ rotamer and those of Phe^7 and Lys^9 are in the gauche$^+$ rotamer (Table S1). Hence, the side chains of DPhe^2, Phe^7, and DTrp^8 are in the plane of the backbone of the analogue, whereas the side chain of Lys^9 is pointing away from the plane of the peptide backbone. In all of the 20 conformers calculated, there is a hydrogen bond between the amide proton of Lys^9 and the carbonyl of Phe^7. Experimentally observed small temperature coefficient of −0.002 ppm/K for the amide proton of Lys^9 suggests that it could be involved in a hydrogen bond.

3D Structure of H-Cpa^2-c[DHcy^3-Tyr^7-DTrp^8-Lys^9-Thr^{10}-Hcy^{14}]-Nal^{15}-NH$_2$ (5). Analogue **5** differs from **3** by Cpa at position 2, DHcy at position 3, Tyr at position 7, and Nal at position 15 and has completely lost its binding affinity to receptor 2 (Table 1). The backbone of this analogue has an inverse γ-turn around residue DTrp^8 (Table S1), different from **3** and also from other octreotide-based agonists and antagonists. The torsion angles show that the side chains of Cpa^2, Tyr^7, DTrp^8, Lys^9, and Nal^{15} are in the gauche$^+$ rotamer. This configuration orients the side chains of Tyr^7, DTrp^8, Lys^9, and Nal^{15} in the plane of the peptide backbone, and the side chain of Cpa^2 is oriented away from the plane of the backbone (Figure 2). No hydrogen bond stabilizing the structure is observed in all of the 20 conformers calculated.

Discussion

Influence of the Ring Size on Receptor Binding Affinity. Comparing the three analogues studied from a structural, chemical, and biological point of view, it is observed that the number of atoms in the disulfide bridge had a major impact on both the conformation and the receptor selectivity. The introduction of Ncy in the octreotide-based sst$_2$ agonist (**1**) resulted in **2**. The shorter side chain of Ncy constrained the peptide backbone so tightly that the analogue lost binding affinity to all of the receptors. Introduction of Hcy, which has a longer side chain than Cys, resulted in **3** with partial selectivity for sst$_2$. In contrast, DHcy with a different chirality at position 3 resulted in **5** with a complete loss of binding to sst$_2$. From a structural perspective, Hcy$^{3/14}$ substitutions (**3**, the number of atoms in the cycle changed from 20 to 22 compared to **1**) modify the conformation of the peptide backbone because of the flexibility in the disulfide bridge, thereby slightly changing the relative orientation of the amino acid side chains (Figure 2). But the introduction of DHcy^3 alters the backbone conformation from a type-II β-turn to a γ-turn, thereby significantly changing the relative orientation of the amino acid side chains (Figure 2). All of these observations support the fact that the backbone conformation is not responsible for the binding of peptides; it rather acts as a scaffold in orienting the side chains of the analogues to interact efficiently with the receptor. Hence, the spatial orientation of the amino acid side chains for the analogues is compared with the sst$_2$-selective pharmacophore in the following section.

Comparison of the 3D Structures of 3 and 5 with the sst$_2$-Selective Pharmacophore. The sst$_2$-selective pharmacophore requires one aromatic side chain far from the side chains of DTrp^8−Lys^9, as shown in Figure 3[4] and Table 3. Figure 3 shows octreotide in two different conformations, and the one shown in magenta represents the structure required for the sst$_2$-selective pharmacophore. Analogue **3** binds to sst$_2$ with the affinity of

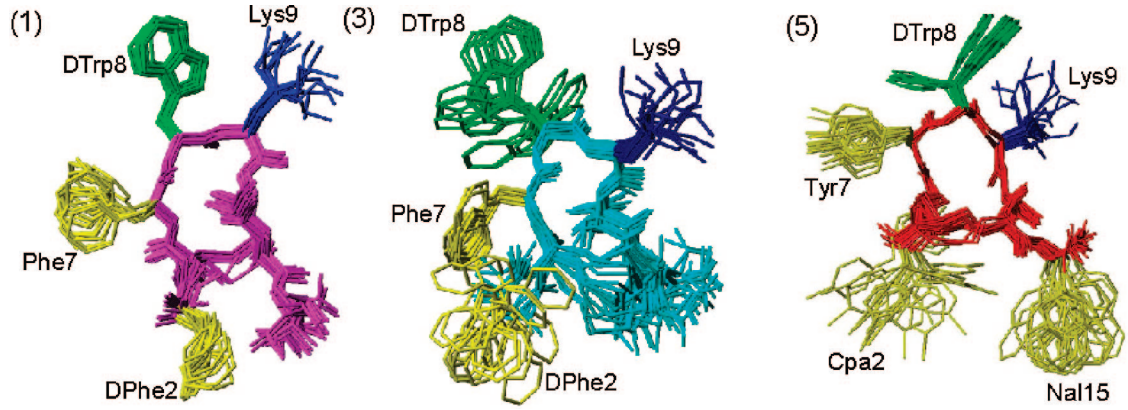

Figure 2. 3D structures of **1**, **3**, and **5** studied by NMR. For each analogue, 20 energy-minimized conformers with the lowest target function are used to represent the 3D NMR structure. The bundle is obtained by overlapping the C^{α} atoms of all the residues. The backbone and the side chains are displayed, including the disulfide bridge. The following color code is used: magenta, (**1**) H-DPhe-c[Cys-Phe-DTrp-Lys-Thr-Cys]-Thr-NH_2; cyan, (**3**) H-DPhe-c[Hcy-Phe-DTrp-Lys-Thr-Hcy]-Thr-NH_2; and red, (**5**) H-Cpa-c[DHcy-Tyr-DTrp-Lys-Thr-Hcy]-Nal-NH_2. The amino acid side chains which are proposed to be involved in binding to the various SRIF receptors are highlighted: light green, DTrp at position 8; blue, Lys at position 9; and yellow, DPhe or Cpa at position 2, Phe or Tyr at position 7, and Nal at position 15.

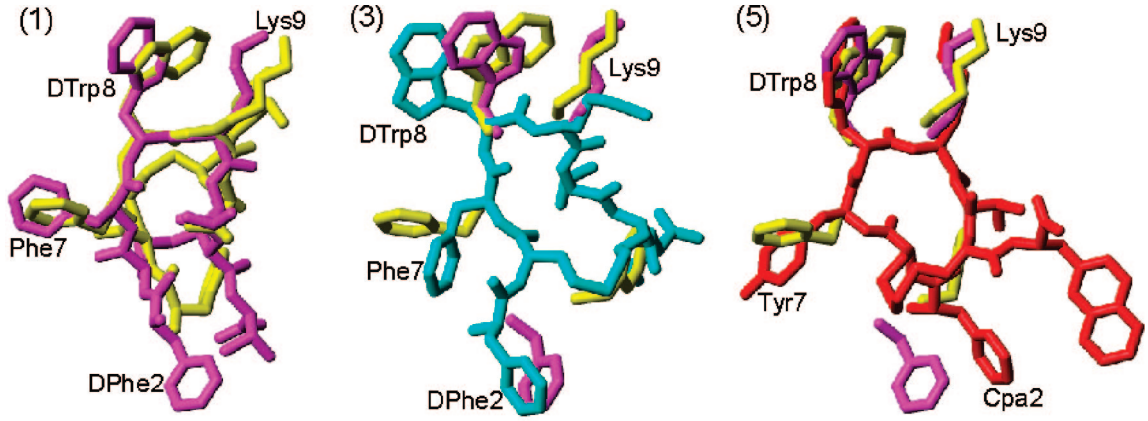

Figure 3. Superposition of receptor-specific pharmacophores of octreotide with the 3D NMR structures of **3** and **5**. The sst_2 pharmacophore[4] of octreotide is shown in magenta. The octreotide pharmacophore proposed by Melacini et al.[3] is represented in yellow. For both pharmacophores, only the amino acid side chains that are involved in binding to the receptor are shown. For each of the analogues **3** and **5,** the conformer with the lowest energy is used to represent the 3D structure of the analogue. The analogues are colored as in Figure 2, and for each analogue, the amino acid side chains proposed to be involved in receptor binding are labeled for clarity.

Table 3. Distances between Cγ Atoms (in Å) of Selected Residues in the Different Pharmacophores Compared with those Found in the Analogues Studied by NMR

analogue	F^2-F^7	$F^2-{}^DW^8$	F^2-K^9	$F^7-{}^DW^8$	F^7-K^9	$^DW^8-K^9$
sst_2 pharmacophore[4]		12.0−13.5	12.5−15.0			4.0−5.0
octreotide pharmacophore[1]	5.0−11.0	11.0−15.0	12.0−15.0	7.0−9.0	9.0−11.0	5.0−5.0
1	8.1−9.9	13.5−14.6	13.5−14.8	6.7−8.0	10.0−11.2	5.3−5.7
3	6.3−8.9	10.9−14.3	11.9−14.9	5.5−7.0	9.5−10.1	6.8−8.1
5	8.6−10.3	11.5−14.6	9.6−13.7	4.3−7.2	10.2−10.7	6.3−7.6

4.9 nM, and the 3D NMR structure of this analogue in DMSO shows that it prefers a conformation which has the sst_2-selective pharmacophore (Figure 3). Analogue **3** has the type-II′ β-turn similar to the sst_2-selective analogues, and the side chains of $DPhe^2$, $DTrp^8$, and Lys^9 are in the plane of the backbone of the analogue, just like in **1** (Figure 3). The flexibility in the side chain of $DPhe^2$ along with the backbone flexibility due to the longer Hcy at positions 3 and 14 explains the low binding affinity of this analogue to sst_4 and sst_5 receptors. Analogue **5**, with DHcy at position 3, has an inverse γ-turn around residue $DTrp^8$. Superimposing the structure of **5** on that of octreotide shows that the side chain of Cpa^2 lies in between sst_2- and sst_5-selective pharmacophores (Figure 3). Because of the available conformational flexibility in the backbone of the analogue with DHcy at position 3 and Hcy at position 14, one would expect the aromatic side chain of Cpa^2 to fit both sst_2 and sst_5pharmacophores. The binding data of **5** compared to those of **4** show a 50-fold loss of binding affinity to sst_2, equal affinity to sst_5, a 3-fold loss to sst_3, and some gain of binding affinity to sst_1 and sst_4 (Table 1). Hence, the binding data could only be explained on the basis of the 3D structure, which shows that the bulkier Nal group at the C-terminus extends further away in the plane of the peptide backbone, which probably prevents the analogue from binding to both sst_2 and sst_5. Analogues **4** and **5** are antagonists at sst_2 on the basis of their ability to inhibit the [Tyr^3]octreotide-induced sst_2 internalization. The 3D NMR structures of antagonist analogues very similar to that of analogue **4** show that the position of the aromatic side chain at

position 2 is very crucial for sst_2 binding. In addition, the position of the Nal group at the C-terminus is within the framework of the peptide backbone for most of the analogues.[15]

Conclusions

The synthesis, binding, and 3D NMR structural characterization of octreotide-based analogues with different numbers of atoms in the cysteine side chain involved in the disulfide bond is reported. Reducing the number of atoms by using Ncy resulted in tremendous loss in binding affinity because of the restriction in the backbone flexibility. Increasing the number of atoms in the cycle had different effects for the agonist and the antagonist. Although Hcy at position 3 enhanced selectivity for sst_2, DHcy replacement at position 3 resulted in dramatic loss in affinity compared to the parent compound. The 3D NMR structures identified the presence and absence of the sst_2-selective pharmacophore in the analogues, which explains the binding data. The current data highlight the indirect role of changes in size of the disulfide bridge in inducing the backbone conformation, which in turn, orients the side chains of the residues involved in receptor interaction.

Experimental Section

Functional Studies: Receptor Internalization. Immunofluorescence microscopy-based internalization assays with HEK-sst_2 cells were performed as previously described by Cescato et al.[16] Briefly, cells were treated either with [Tyr^3]-octreotide, **1**, **3**, **4**, or **5** at concentrations ranging from 100 to 10−000 nM or, to evaluate potential antagonism, with 100 nM [Tyr^3]-octreotide in the presence of a 100-fold excess of **1**, **3**, **4**, or **5** for 30 min at 37 °C and 5% CO_2 in growth medium and then processed for immunofluorescence microscopy by using the polyclonal sst_2-specific R2-88 antibody (provided by Dr. A. Schonbrunn, University of Texas Medical School, Houston, TX) at a dilution of 1:1000 as first antibody and Alexa Fluor 488 goat antirabbit IgG (H + L) at a dilution of 1:600 as secondary antibody. The cells were imaged as described previously.[16]

NMR Studies. NMR samples were prepared by dissolving 2 mg of the analogue in 0.5 mL of DMSO-d_6. The ^{1}H NMR spectra were recorded on a Bruker 700 MHz spectrometer operating at a proton frequency of 700 MHz. Chemical shifts were measured by using DMSO (δ = 2.49 ppm) as an internal standard. The 1D spectra and all the 2D spectra were acquired at 298 K. Resonance assignments of the various proton resonances were carried out by using total correlation spectroscopy (TOCSY);[17,18] double quantum filtered spectroscopy (DQF-COSY)[19] and NOESY.[20–22] The TOCSY experiments employed the MLEV-17 spin-locking sequence suggested by Davis and Bax,[17] applied for a mixing time of 50 ms. The NOESY experiments were carried out with a mixing time of 100 ms. The TOCSY and NOESY spectra were acquired by using 800 complex data points in the ω_1 dimension and 1024 complex data points in the ω_2 dimension, with t_{1max} = 33 ms and a t_{2max} = 43 ms, and were subsequently zero-filled to 1024 × 2048 before Fourier transformation. The DQF-COSY spectra were acquired with 1024 × 4096 data points and were zero-filled to 2048 × 4096 before Fourier transformation. The TOCSY, DQF-COSY, and NOESY spectra were acquired with 8, 8, and 16 scans, respectively, with a relaxation delay of 1 s. The signal from the residual water of the solvent was suppressed by using presaturation during the relaxation delay and during mixing time. The TOCSY and NOESY data were multiplied by 75°-shifted sine function in both dimensions. All the spectra were processed by using the software PROSA.[23] The spectra were analyzed by using the software X-EASY.[24]

Structure Determination. The chemical shift assignment of the major conformer (the population of the minor conformer was <10%) was obtained by the standard procedure by using DQF-COSY and TOCSY spectra for intraresidual assignment, and the NOESY spectrum was used for the sequential assignment.[25] The collection of structural restraints was based on the NOEs assigned manually and vicinal $^3J_{NH\alpha}$ couplings. Dihedral angle constraints were obtained from the $^3J_{NH\alpha}$ couplings, which were measured from the 1D ^{1}H NMR spectra and from the intraresidual and sequential NOEs, along with the macro GRIDSEARCH in the program CYANA.[13] The calibration of NOE intensities versus ^{1}H−^{1}H distance restraints and appropriate pseudoatom corrections to the nonstereospecifically assigned methylene, methyl, and ring protons were performed by using the program CYANA. On average, approximately 100 NOE constraints and 15−20 angle constraints were utilized to calculate the conformers (Table 2). A total of 100 conformers was initially generated by CYANA, and a bundle containing 20 CYANA conformers with the lowest target function values were utilized for further restrained energy minimization by using the program DISCOVER with steepest decent and conjugate gradient algorithms.[26] The resulting energy-minimized bundle of 20 conformers was used as a basis for discussing the solution conformation of the different SRIF analogues. The structures were analyzed by using the program MOLMOL.[27]

Acknowledgment. This work was supported in part by NIH grant R01 DK059953. We are indebted to R. Kaiser and C. Miller for technical assistance in the synthesis and characterization of the peptides. We thank Dr. W. Fisher and W. Low for mass spectrometric analyses of the analogues and D. Doan for manuscript preparation. J.R. is the Dr. Frederik Paulsen Chair in Neurosciences Professor.

Supporting Information Available: Starting materials, peptide synthesis, cleavage and deprotection with HF and cyclization, purification and chemical characterization of the analogues, cell culture, and receptor binding data are reported in Supporting Material. Similarly, Table S1 (torsion angles φ, Ψ, and χ_1 (in °) of the bundle of 20 energy-minimized conformers) and Table S2 (proton chemical shifts of the analogues studied by NMR) are reported in Supporting Material. This material is available free of charge via the Internet at http://pubs.acs.org.

References

(1) Melacini, G.; Zhu, Q.; Goodman, M. Multiconformational NMR analysis of sandostatin (octreotide): Equilibrium between β-sheet and partially helical structures. *Biochemistry* **1997**, *36*, 1233–1241.
(2) Osapay, G.; Prokai, L.; Kin, H.-S.; Medzihradszky, K. F.; Coy, D. H.; Liapakis, G.; Reisine, T.; Melacini, G.; Zhu, Q.; Wang, S. H.-H.; Mattern, R.-H.; Goodman, M. Lanthionine-somatostatin analogs: Synthesis, characterization, biological activity, and enzymatic stability studies. *J. Med. Chem.* **1997**, *40*, 2241–2251.
(3) Melacini, G.; Zhu, Q.; Osapay, G.; Goodman, M. A refined model for the somatostatin pharmacophore: Conformational analysis of lanthionine-sandostatin analogs. *J. Med. Chem.* **1997**, *40*, 2252–2258.
(4) Grace, C. R. R.; Erchegyi, J.; Koerber, S. C.; Reubi, J. C.; Rivier, J.; Riek, R. Novel sst_2-selective somatostatin agonists. Three-dimensional consensus structure by NMR. *J. Med. Chem.* **2006**, *49*, 4487–4496.
(5) Bass, R. T.; Buckwalter, B. L.; Patel, B. P.; Pausch, M. H.; Price, L. A.; Strnad, J.; Hadcock, J. R. Identification and characterization of novel somatostatin antagonists. *Mol. Pharmacol.* **1996**, *50*, 709–715.
(6) Samant, M. P.; Rivier, J. E. Norcystine, a new tool for the study of the structure−activity relationship of peptides. *Org. Lett.* **2006**, *8*, 2361–2364.
(7) Erchegyi, J.; Grace, C. R. R.; Samant, M.; Cescato, R.; Piccand, V.; Riek, R.; Reubi, J. C.; Rivier, J. E. Ring size of somatostatin analogues (ODT-8) modulates receptor selectivity and binding affinity. *J. Med. Chem.* **2008**, *51*, 2668–2675.
(8) Erchegyi, J.; Hoeger, C. A.; Low, W.; Hoyer, D.; Waser, B.; Eltschinger, V.; Schaer, J.-C.; Cescato, R.; Reubi, J. C.; Rivier, J. E. Somatostatin receptor 1 selective analogues: 2. N-methylated scan. *J. Med. Chem.* **2005**, *48*, 507–514.
(9) Miller, C.; Rivier, J. Peptide chemistry: Development of high-performance liquid chromatography and capillary zone electrophoresis. *Biopolym. Pept. Sci.* **1996**, *40*, 265–317.
(10) Miller, C.; Rivier, J. Analysis of synthetic peptides by capillary zone electrophoresis in organic/aqueous buffers. *J. Pept. Res.* **1998**, *51*, 444–451.

(11) Reubi, J. C.; Schaer, J. C.; Waser, B.; Wenger, S.; Heppeler, A.; Schmitt, J. S.; Mäcke, H. R. Affinity profiles for human somatostatin receptor sst1-sst5 of somatostatin radiotracers selected for scintigraphic and radiotherapeutic use. *Eur. J. Nucl. Med.* **2000**, *27*, 273–282.

(12) Reubi, J. C.; Schaer, J. C.; Waser, B.; Hoeger, C.; Rivier, J. A selective analog for the somatostatin sst1-receptor subtype expressed by human tumors. *Eur. J. Pharmacol.* **1998**, *345*, 103–110.

(13) Güntert, P.; Mumenthaler, C.; Wüthrich, K. Torsion angle dynamics for NMR structure calculation with the new program DYANA. *J. Mol. Biol.* **1997**, *273*, 283–298.

(14) Hagler, A. T.; Dauber, P.; Osguthorpe, D. J.; Hempel, J. C. Dynamics and conformational energetics of a peptide hormone: Vasopressin. *Science* **1985**, *227*, 1309–1315.

(15) Cescato, R.; Grace, C. R. R.; Erchegyi, J.; Waser, B.; Piccand, V; Mäcke, H. R.; Riek, R.; Rivier, J. E.; Reubi, J. C. Design, structure and in vitro characterization of highly sst_2-selective somatostatin antagonists suitable for radio-targeting. *J. Med. Chem.* 2008, submitted.

(16) Cescato, R.; Schulz, S.; Waser, B.; Eltschinger, V.; Rivier, J. E.; Wester, H. J.; Culler, M.; Ginj, M.; Liu, Q.; Schonbrunn, A.; Reubi, J. C. Internalization of sst_2, sst_3, and sst_5 receptors: Effects of somatostatin agonists and antagonists. *J. Nucl. Med.* **2006**, *47*, 502–511.

(17) Davis, D. G.; Bax, A. Assignment of complex ^{1}H NMR spectra via two-dimensional homonuclear Hartmann-Hahn spectroscopy. *J. Am. Chem. Soc.* **1985**, *107*, 2820–2821.

(18) Braunschweiler, L.; Ernst, R. R. Coherence transfer by isotropic mixing: Application to proton correlation spectroscopy. *J. Magn. Reson.* **1983**, *53*, 521–528.

(19) Rance, M.; Sorensen, O. W.; Bodenhausen, B.; Wagner, G.; Ernst, R. R.; Wüthrich, K. Improved spectral resolution in COSY ^{1}H NMR spectra of proteins via double quantum filtering. *Biochem. Biophys. Res. Commun.* **1983**, *117*, 479–485.

(20) Kumar, A.; Wagner, G.; Ernst, R. R.; Wüthrich, K. Buildup rates of the nuclear Overhauser effect measured by two-dimensional proton magnetic resonance spectroscopy: Implications for studies of protein conformation. *J. Am. Chem. Soc.* **1981**, *103*, 3654–3658.

(21) Macura, S.; Ernst, R. R. Elucidation of cross-relaxation in liquids by two-dimensional NMR spectroscopy. *Mol. Phys.* **1980**, *41*, 95–117.

(22) Macura, S.; Huang, Y.; Suter, D.; Ernst, R. R. Two-dimensional chemical exchange and cross-relaxation spectroscopy of coupled nuclear spins. *J. Magn. Reson.* **1981**, *43*, 259–281.

(23) Güntert, P.; Dotsch, V.; Wider, G.; Wüthrich, K. Processing of multi-dimensional NMR data with the new software PROSA. *J. Biolmol. NMR* **1992**, *2*, 619–629.

(24) Eccles, C.; Güntert, P.; Billeter, M.; Wüthrich, K. Efficient analysis of protein 2D NMR spectra using the software package EASY. *J. Biomol. NMR* **1991**, *1*, 111–130.

(25) Wüthrich, K. *NMR of Proteins and Nucleic Acids*; J. Wiley & Sons: New York, 1986.

(26) Hagler, A. T. Theoretical simulation of conformation, energetics and dynamics of peptides. *The Peptides: Analysis, Synthesis, Biology*; Academic Press: Orlando, FL, 1985; pp 213–299.

(27) Koradi, R.; Billeter, M. MOLMOL: A program for display and analysis of macromolecular structures. *PDB Newsletter* **1998**, *84*, 5–7.

(28) Hocart, S. J.; Jain, R.; Murphy, W. A.; Taylor, J. E.; Coy, D. H. Highly potent cyclic disulfide antagonists of somatostatin. *J. Med. Chem.* **1999**, *42*, 1863–1871.

JM701445Q